Threshold and Ablation Efficiency Studies of Microsecond Ablation of Gelatin Under Water

Ujwal S. Sathyam, MS, Alan Shearin, BS, Edward A. Chasteney, MD, and Scott A. Prahl, PhD

Oregon Graduate Institute, Portland, Oregon 97291 (U.S.S., S.A.P.) Oregon Medical Laser Center, Portland, Oregon 97225 (U.S.S., A.S., E.A.C., S.A.P.) Oregon Health Sciences University, Portland, Oregon 97201 (E.A.C., S.A.P.) Palomar Medical Technologies, Inc., Beverly, Massachusetts 01915 (A.S.)

Background and Objective: Laser thrombolysis is the selective ablation of thrombus occluding vessels by microsecond pulsed laser irradiation. To achieve efficient ablation of thrombus, the optimal wavelength, spot size, and pulse energy need to be determined.

Study Design/Materials and Methods: A gelatin-based thrombus model confined in 3 mm inner diameter tubes was ablated under water using a 1 μs pulsed dye laser. Wavelength studies were conducted by varying the absorption of the gelatin between 10–2000 cm^{-1} corresponding to the waveband between 400–600 nm on the absorption spectrum of thrombus. A unique spectrophotometric method was developed to measure the ablated mass. An acoustic method was used to measure ablation thresholds under water as a function of absorption.

Results: The mass removed per pulse per unit energy was nearly equal over an absorption range of 100–1000 cm^{-1} at pulse energies above threshold. Mass removal increased linearly with pulse energy but did not have a direct relationship with radiant exposure. Ablation thresholds indicate that the gelatin needed to be heated only to 100°C for ablation to commence. Ablation masses measured were an order of magnitude higher than those predicted by thermal ablation models.

Conclusion: The results suggest that any wavelength between 410–590 nm can be used for effective thrombolysis. The ablation efficiency depends on the total energy delivered rather than the radiant exposure. The high ablation efficiencies suggest a dominance of the mechanical action of vapor bubbles over thermal ablation in the ablation process. © 1996 Wiley-Liss, Inc.

Key words: absorption, artery, blood, bubble, cavitation, energy, radiant exposure, thrombolysis, thrombus, wavelength

INTRODUCTION

Ablation of arterial obstructions by pulsed laser radiation has emerged as a potential method to recanalize vessels occluded by plaque and thrombus [1–3]. In an effort to optimize the procedure, there have been numerous parametric studies of ablation of plaque using lasers ranging in wavelength from the ultraviolet to the infrared and in pulse width from less than 100 ns to more than 100 μs [4–9]. However, the ablation of thrombus is still a largely unresolved issue. Since arterial obstructions are usually a combination of plaque and thrombus, ablation of thrombus would expose the underlying plaque for subsequent therapy. Laser thrombolysis may also prove to be

a viable method of clearing thrombosed bypass grafts.

A primary advantage of laser thrombolysis over other recanalization techniques is the potential for selective removal of thrombus without incurring injury to the adjacent arterial tissue. This can be achieved by choosing a laser wavelength which is well absorbed by the thrombus but not by the vessel wall. LaMuraglia et al. showed that thrombus absorbs light much more than the vessel wall in the 400–600 nm due waveband to the presence of hemoglobin (Fig. 7) [10,11]. Current investigations of laser thrombolysis have made use of tunable pulsed-dye lasers operating at 490 nm and 577 nm with pulse lengths of 1–2 μs [3,10]. However, the best wavelength for efficient ablation in the 400–600 nm waveband is not known. No complete parametric study of microsecond ablation of a soft target under a liquid has been undertaken yet.

The aims of this study were to optimize laser parameters such as wavelength, spot size, and pulse energy for efficient ablation. The choice of wavelength determines the absorption coefficients of blood, thrombus, and artery. Since the ablation threshold for a tissue depends on its absorption coefficient, we also wanted to establish the relationship between the ablation threshold radiant exposure and absorption coefficient. This would help in setting an optimal radiant exposure for efficient ablation without injury to the vessel wall at any wavelength. The spot size is important in determining the size of the catheter delivering the laser energy.

Since the wavelength determines the penetration depth into the tissue, it has been theorized that an optimal wavelength for laser thrombolysis would be found at an optimal penetration depth. Early studies have speculated that deeper penetrating wavelengths in the 400–600 nm waveband would result in higher ablation efficiency since a larger volume would be heated [10]. Later studies suggested that primarily the 410 nm and to a lesser extent the 450–500 nm wavelengths were among the most effective for laser thrombolysis since they provided the highest degree of selectivity in absorption between thrombus and vessel wall [11]. However, there is no experimental evidence available to positively justify the choice of a particular wavelength. The question then arises: How important is light absorption in mass removal at energies above threshold? Laser thrombolysis is done in a fluid medium, and an important phenomenon influenc-

ing removal of tissue under a liquid is cavitation or the formation and collapse of a vapor bubble [12–14]. The contribution of the bubble dynamics to the ablation process may be comparable to or even overshadow the absorption-dependent thermal effects. It is therefore important to estimate the relative significance of the absorption coefficient in the ablation process at energies above threshold.

This study investigated the effects of absorption and radiant exposure on the ablation efficiency of a gelatin-based thrombus model under flowing water. The use of the thrombus model eliminated the biological variability of thrombus. Since thrombolysis is performed under an aqueous medium of saline and contrast, the gelatin was ablated under water. An important aspect of laser thrombolysis is the constraining cylindrical geometry of the vessel wall. In our experiments, the gelatin was confined in plastic tubes to simulate the cylindrical boundaries of the arterial wall. We developed a unique spectrophotometric method to accurately measure the ablated mass within 5%. Thresholds for ablation under water were measured as a function of absorption coefficient. An absorption range of 10–2000 cm^{-1} was studied which corresponded to the waveband between 400–600 nm on the absorption spectrum of thrombus. The radiant exposure was varied by varying both the pulse energy and irradiated spot size, and ablation efficiency was characterized as the amount of gelatin ablated per pulse per unit energy.

The results of our study indicate that absorption has little effect on the ablation efficiency at energies above threshold. This implies that laser thrombolysis can be done at most visible wavelengths. The ablation efficiency remains constant with pulse energy and has no direct relationship with radiant exposure. The ablated masses were nearly an order of magnitude higher than the vaporized volumes calculated based on thermal models. This indicates the importance of the mechanical action of the vapor bubble in the ablation process. Ablation thresholds indicate that the tissue surface has to be heated to only 100°C for ablation to take place.

MATERIALS AND METHODS
Preparation of Thrombus Models

The thrombus was modeled using a 3.5% gelatin (175 Bloom) containing a photostable absorbing dye as the chromophore (Direct Red 81 from
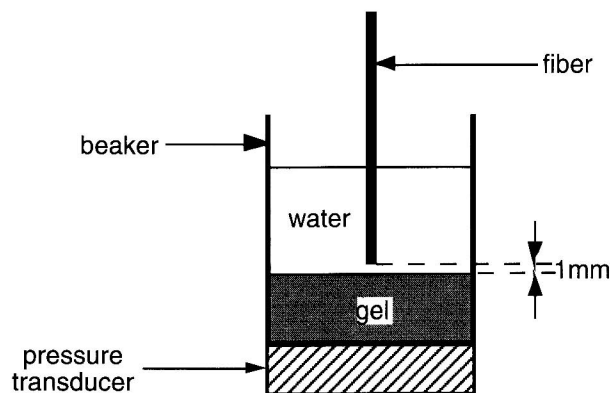
Fig. 1. Ablation thresholds are measured by detecting an acoustic signal accompanying ablation. Light is delivered in 1 μs pulses, and the energy is increased until an acoustic signal is observed.

Sigma). The gelatin-water mixture was heated to 60°C and sufficient chromophore was added to achieve the desired absorption coefficient at the laser wavelength used. The absorption coefficients of the samples had a linear relationship with the concentration of chromophore in the gelatin solution: 0.089g of chromophore in a solution of 1.4g gelatin and 40 cm^3 water gave an absorption coefficient of 100 cm^{-1} at 577 nm. The absorption coefficients ranged from 10 cm^{-1} to 2000 cm^{-1}.

A 1 μs pulsed dye laser (Palomar Medical Technologies, Beverly, MA) operating at a wavelength 577 nm was used for ablation. Quartz fibers of 300, 600, and 1000 μm core diameter were used to deliver the laser pulses to the gelatin targets.

Measurement of Threshold Radiant Exposure

Ablation threshold energies at absorption coefficients from 10–1000 cm^{-1} were determined by detecting an acoustic signal accompanying ablation in a semi-infinite medium under water (Fig. 1). Gel samples were prepared in a 250 ml beaker to form a 1 cm thick layer and covered with water. The beaker was then placed on a PVDF transducer (Hydrosonics) connected to a digital signal analyzer (Tektronix DSA 602A) through an amplifier (Hydrosonics).

Laser pulses were delivered from a distance of 1 mm to the gel surface via a 1000 μm fiber, and explosive ablation was accompanied by an acoustic signal which was detected by the transducer. The threshold energy was the pulse energy required to produce a signal of 30 mV peak-peak on the signal analyzer. A value of 30 mV was chosen

because it was the minimum signal differentiable from the background noise. Since this method was based on the assumption that the acoustic signal was the result of an ablation event, validation of the method by mass removal experiments was essential. The results were verified by ablating the gelatin in 3 mm diameter tubes and comparing the mass removals at pulse energies below and above the acoustically measured threshold energies.

Each pulse was fired on a fresh target area to maintain surface geometry and fiber-to-target distance. Five measurements were taken for each absorption coefficient and radiant exposures were calculated by dividing the threshold energy by the spot size on the gelatin surface. Ablation threshold energies for 300 cm^{-1} gels were also determined using 300 μm and 600 μm fibers and threshold radiant exposures were calculated.

Ablation of Gelatin in Tubes

Liquid gelatin samples were drawn up into 3 mm inner diameter tubes (Tygon) and cured to form 1–2 cm long thrombus models (Fig. 2). Light was delivered through a solid glass fiber with its tip about 1 mm from the gel surface. A steady flow of water at 0.3 ml/s was established by a fluid injector (Medrad Mark V) and directed around the fiber to target site. Ten pulses at a rate of 3 Hz were fired on each sample and the ablated gel was collected by the flowing water in 1 cm cuvettes. The steady flow was continued after the last pulse until 4 ml of liquid was collected which was sufficient to collect all the ablated gel. The above procedure was repeated on control samples without light delivery to account for the gel removed by the flow of water alone. The ablated gel was dissolved completely in the water by shaking, and its mass was determined by the spectrophotometric method described below. The ablation efficiency was then calculated as the mass removed per unit energy per pulse.

Absorption studies were conducted by delivering pulse energies of 25–100 mJ via a 1000 μm fiber to gels with absorptions varying from 10–2000 cm^{-1}. Radiant exposure studies were conducted by delivering pulse energies of 25–100 mJ via 300, 600, and 1000 μm fibers to gels with an absorption of 300 cm^{-1}. An absorption of 300 cm^{-1} was chosen in the radiant exposure studies since thrombus has this absorption at 577 nm which is one of the wavelengths used in clinical trials of laser thrombolysis.

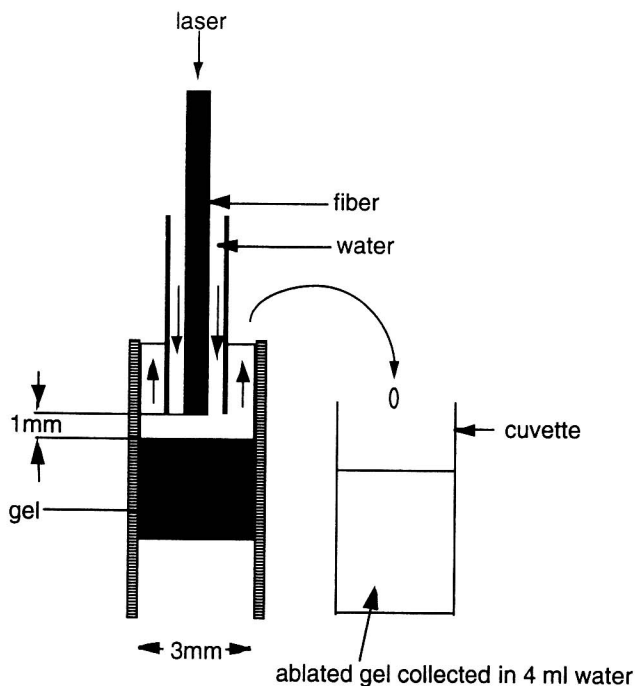Ten samples and five controls were used for

Fig. 2. Gelatin containing an absorbing dye is confined in a 3 mm diameter tube. Laser energy is delivered in 1 μs pulses via a solid glass fiber at a distance of 1 mm to the gelatin. The ablated material is collected in 4 ml water and the absorbance is measured in a spectrophotometer.
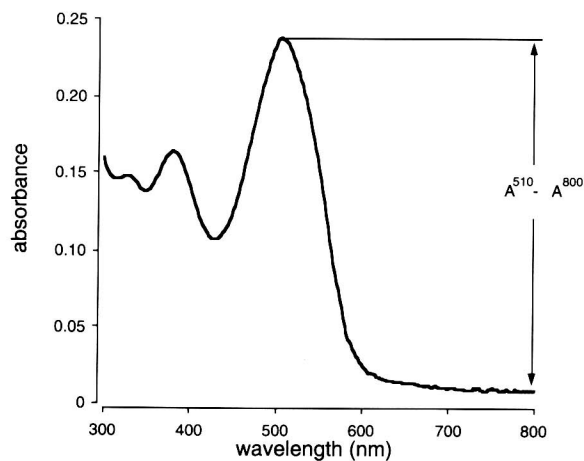

Fig. 3. Direct Red absorption spectrum: The difference in absorbances at 510 nm and 800 nm of the ablated gelatin in solution gives a measure of its dye content from which the total mass of ablated material can be determined. Absorbance represented here was measured in a 1 cm cuvette with 6 μg/ml dye concentration in water.

each data point. Pulse energies were measured with a joulemeter (Molectron). The effective spot sizes produced 1 mm from fiber end were determined by ablating fiber polishing paper under water and measuring the resulting burn diameters under a microscope.

Spectrophotometric Measurement of Ablation Mass

Since the mass of the ablated material was very small and ablation took place in a fluid environment, conventional methods of measuring mass were not suitable. We therefore devised a method in which the absorbance of the solution was compared with the absorbance of a known concentration of dye solution to determine the mass of the ablated gel.

A calibration curve was established by measuring the difference in absorbances at 510 nm and 800 nm as measured on a spectrophotometer (HP 8452A) for a range of dye masses in 4 ml of water. The dye has its maximum absorption peak at 510 nm, and the 800 nm wavelength corresponded to low background absorption (Fig. 3). The two wavelength method minimized errors due to low concentrations of dye and variability in

the plastic cuvettes. The resulting error estimates in absorbance were less than 5% at any dye mass. The linear relationship between absorbance and mass of dye in 4 ml water served as a calibration for future measurements of ablation masses. The slope of our calibration line was determined to be 0.01/μg.

The difference in absorbances between 510 nm and 800 nm of the ablated gel in solution was measured and the amount of dye in the gel was determined from the calibration experiment. Since the exact amount of dye which went into the gel preparation was known, the amount of material ablated was calculated using:

total mass ablated

$$= \frac{(A_s^{510} - A_s^{800}) - (A_c^{510} - A_c^{800})}{\text{slope of calibration line}} \times \frac{M_w + M_g + M_d}{M_d}$$

where A^{510} and A^{800} are the absorbances at 510 nm and 800 nm respectively. Subscripts 's' and 'c' refer to laser ablated samples and controls. M_w, M_g, and M_d are the masses of water, gelatin, and dye used for gel preparation. The first term on the right side of the equation gives the amount of dye in the ablated material, while the second term converts the mass of dye to the total ablated mass. A direct correlation to the calibration experiment is possible since the ablated material was also collected in 4 ml of water. Corrections due to material collected by washing, given by the control

samples, were made as indicated in the above equation and the ablation mass for each absorption coefficient and laser energy was calculated as the average mass ablated per laser pulse.

RESULTS

Ablation of gelatin was characterized by a snapping sound and visible removal of material. The ablated gelatin was removed in very small chunks which quickly dissolved in the water. All the ablated material was collected in the mass removal experiments. The spectrophotometric method of measuring the ablation mass proved accurate and reproducible with an error estimate of less than 5%. An increase in crater depth with multiple pulses was observed. Control samples showed that gelatin collected by the washing action alone typically accounted for less than 3% of the total mass removed.

Threshold Radiant Exposure

Threshold radiant exposures ranged from 160 ± 10 mJ/mm^2 at 10 cm^{-1} to 8.5 ± 0.5 mJ/mm^2 at 1000 cm^{-1} (Fig. 4). Gross visual examination of the gelatin surface revealed craters at energies that produced an acoustic signal. Some surface deformation was observed in a few cases at energies below the designated threshold indicating minimal material removal. The threshold values obtained were validated by spectrophotometric mass loss experiments using Tygon tubes at absorption coefficients of 10, 100, and 1000 cm^{-1}. Threshold was designated as the energy at which mass loss commenced. The values obtained by the two methods at these absorption coefficients are shown in Table 1 and agree favorably with each other.

The spot sizes made by 300, 600, and 1000 μm fibers 1 mm from polishing paper under water were measured to be 520, 650, and 1070 μm in diameter respectively. Threshold energies of 4, 7, and 13 mJ were measured using 300, 600, and 1000 μm fibers respectively on 300 cm^{-1} gelatin. The radiant exposure was calculated in each case by dividing the threshold energy by the corresponding spot size. This resulted in a threshold radiant exposure of 18 ± 3 mJ/mm^2.

Ablation of Gelatin in Tubes

Effect of absorption. At pulse energies of 25, 50, and 100 mJ, no material was removed at an absorption coefficient of 10 cm^{-1} (Fig. 5). No snapping sound could be heard and gross visual

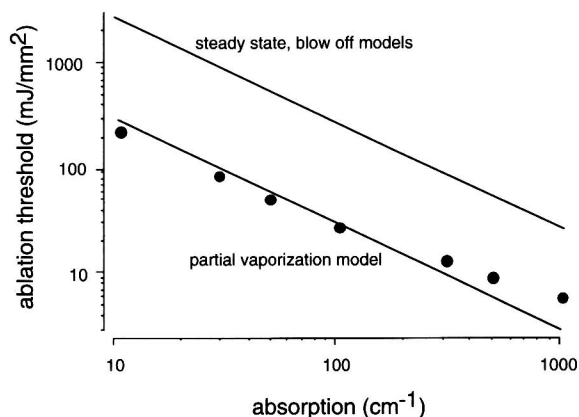Fig. 4. Threshold radiant exposures for gels of different absorption coefficients measured acoustically using a 1000 μm fiber and maintaining a 1 mm distance from the gelatin surface under water. Error bars are smaller than symbols.

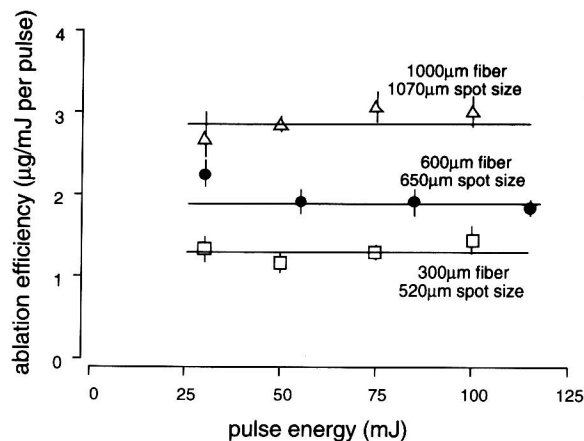examination revealed no craters. Pulse energies of 50–100 mJ resulted in ablation efficiencies of less than 1 μg/mJ at 30 cm^{-1}. Acoustic signals were muted or absent. At higher absorption coefficients the ablation efficiency increased and remained roughly constant between 2–3 μg/mJ from 100–1000 cm^{-1} for all three pulse energies. Ablation in this region was accompanied by a loud snapping sound indicating explosive removal of material. Visual examination of the craters after 10 pulses showed the diameter to be within 10% of the spot size made by the fiber and the depth to vary from 4–6 mm. Above 1000 cm^{-1} the ablation efficiency reduced slightly.

Effect of radiant exposure. More gelatin was removed with larger fibers at the same energy. The 1000 μm fibers ablated about twice as efficiently as 300 μm fibers (Fig. 6). Loud snapping sounds were heard for all the ten pulses fired through the 1000 μm fibers, but the acoustic signals were muted after about five shots using the 300 μm and 600 μm fibers. The ablation efficiency was roughly constant at all pulse energies for a single spot size.

Radiant exposures were calculated by dividing the pulse energy by the spot size made by the fiber. Energies of 50 mJ and 85 mJ through 300 μm and 600 μm fibers respectively produced iso-radiant exposures of about 250 mJ/mm^2, but resulted in different ablation efficiencies. Larger spot sizes resulted in greater ablation efficiencies at similar energies although the radiant exposures were lower.

TABLE 1. Acoustic ablation thresholds were measured by detecting an acoustic signal associated with ablation. These values were validated at three absorptions with mass removal measurements using the spectrophotometric method. Spectrophotometric threshold was defined as the radiant exposure at which mass removal commenced. Fiber diameter was 1 mm with the tip 1 mm from the gel surface. The lines represent the ablation thresholds predicted by the three models.

absorption coefficient (cm^{-1})	spectrophotometric threshold (mJ/mm^2)	acoustic threshold (mJ/mm^2)
10	130 ± 10	160 ± 10
100	14 ± 3	20 ± 1
1000	6 ± 2	8.5 ± 0.5

Fig. 6. Ablation efficiencies at various pulse energies and spot sizes. The squares, circles, and triangles represent 300, 600, and 1000 μm fibers respectively. Absorption coefficient of the gelatin was 300 cm^{-1}. Values are averages of 10 pulses. Error bars denote standard deviation of 10 samples. Lines are visual best fits.
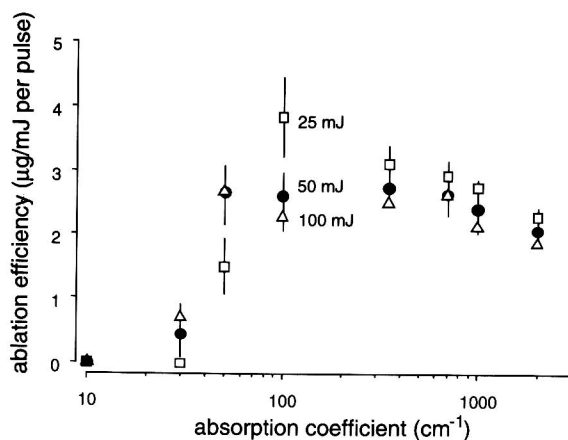
Fig. 5. Ablation efficiency as a function of absorption at different pulse energies. The squares, circles, and triangles represent pulse energies of 25, 50, and 100 mJ respectively. A 1000 μm core diameter glass fiber was used for laser delivery. Values are averages of 10 pulses. Error bars denote standard deviation of 10 samples.

DISCUSSION

This study was carried out to find a suitable wavelength and radiant exposure for microsecond laser ablation of thrombus. Since the choice of wavelength governed the absorption coefficient of thrombus, we investigated the effect of absorption on the ablation efficiency using a gelatin-based thrombus model. The gelatin was ablated in Tygon tubes under water and ablation masses were measured using a spectrophotometric method. To predict ablation threshold for throm-

bus at any wavelength, threshold radiant exposures were determined as a function of absorption coefficient.

We investigated ablation under simulated conditions of cylindrical geometry and present a unique, yet simple method to accurately measure the ablation mass. This method is based on the spectrophotometric signature of the ablated chromophore and allows the effects of various laser parameters and irradiance conditions on ablation under water to be investigated.

Threshold Radiant Exposure

Threshold radiant exposures were determined using a simple method based on detection of an acoustic signal accompanying ablation. Though the signal was potentially degraded by acoustic mismatches at the gelatin-glass and glass-transducer boundaries, the mere presence or absence of a signal was sufficient to differentiate between ablation and non-ablation. No attempt was made to quantitatively analyze the signal. The values obtained using this method were verified independently with mass removal experiments in the Tygon tubes at absorption coefficients of 10, 100, and 1000 cm^{-1}. The close correlation between the threshold radiant exposures using the two methods implies that the onset of ablation is not affected by the geometrical constraints of the tubes. Identical thresholds are not

expected since some of the material in the mass removal experiments could have been removed by melting of the gelatin rather than explosive vaporization.

Measurements with 300, 600, and 1000 μm fibers on 300 cm^{-1} gelatin resulted in nearly equal threshold radiant exposures. This shows that the onset of ablation is governed by radiant exposure and not by energy. The thresholds agree with those found by Prince et al. for microsecond ablation of atheroma and normal aorta at similar absorption coefficients (68 mJ/mm^2 at 54 cm^{-1} and 160 mJ/mm^2 at 26 cm^{-1} respectively) [8]. La-Muraglia et al. reported a threshold radiant exposure of 11 mJ/mm^2 for the ablation of fresh thrombus at a wavelength of 482 nm. The absorption of thrombus at this wavelength is $\sim$100–200 cm^{-1}, and according to the acoustic measurements the threshold radiant exposure for this range lies between 15–20 mJ/mm^2. Evidently, the threshold radiant exposure depends mainly on the absorption coefficient and is relatively independent of material.

Three main theories have been proposed to model ablation of tissue based on heating of the tissue. The steady-state model assumes a steady ablation velocity during the laser pulse [16]. The blow-off model assumes that ablation commences after the laser pulse [17]. Both models describe mass removal in air and assume that the energy required to ablate tissue is that needed to raise the surface temperature to 100°C plus the energy needed for the latent heat of vaporization. Van Leeuwen et al. and Jansen et al. proposed a partial vaporization theory describing bubble formation in a liquid. It predicts that at threshold, the temperature of the liquid needed to be raised to only 100°C [18,19]. Vaporization was then assumed to be initiated at a few nucleation sites. They verified this theory for holmium and excimer ablation.

The experimental threshold values reported in this paper are about an order of magnitude lower than those predicted by both the steady-state and the blow-off models. They are, however, of the same order of magnitude as theoretically calculated by the partial vaporization model. This confirms the theory that the tissue temperature needs to be raised to only 100°C for ablation to commence. It also indicates that ablation is initiated by the formation of a vapor bubble.

Effect of Absorption on Ablation Efficiency

To find an optimal wavelength for laser thrombolysis, we ablated gelatin of various absorption coefficients and measured the mass removed. At low absorption coefficients of 10 cm^{-1}, pulse energies of 25, 50, and 100 mJ (radiant exposures of 28, 56, and 112 mJ/mm^2 respectively) are below ablation threshold since no material was removed. This observation is also confirmed by the acoustic threshold energy measurements which puts the threshold radiant exposure at 160 $\pm$ 10 mJ/mm^2 for 10 cm^{-1}.

The ablation efficiency increases as the absorption increases from a low value of 10 cm^{-1} to about 100 cm^{-1} due to the decreasing threshold energies to below 25 mJ which was the lowest energy used in the ablation mass experiments. However, at 100 cm^{-1} and above, where all three pulse energies used were above threshold, the ablation efficiency remains fairly constant at about 2.5 μg/mJ. The slight decrease in efficiency at high absorptions may be the result of overheating the target material. The comparable mass removal between 100–1000 cm^{-1} indicates that ablation efficiency does not strongly depend on the optical penetration depth (10–100 μm) at energies above threshold.

This has a direct implication for the choice of wavelength for laser thrombolysis as seen in Figure 7, with the caveat that a change in ablation efficiency can be expected due to the different mechanical strengths of thrombus and gelatin. Thrombus has an absorption range of 100–1000 cm^{-1} in the waveband between 410–590 nm, and therefore any wavelength in this range can be chosen without significantly compromising the efficiency. Selectivity would still be retained for radiant exposures below 150 mJ/mm^2 since vessel wall absorption is less than 10 cm^{-1} in this waveband.

Though the threshold is dependent on the absorption coefficient, the total mass removal is fairly independent of absorption at energies above threshold. Both the steady-state and blow-off models predict a strong dependence of the mass removal on the absorption coefficient [16,17]. This implies that thermal ablation is not the dominant factor in the ablation process under a liquid. This suggests that the dominant factor in mass removal under a liquid is some mechanical action which is most likely the result of expansion and/or collapse phases of the vapor bubble.
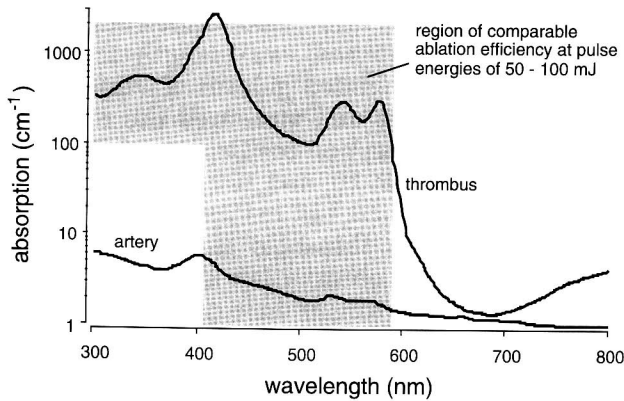
Fig. 7. Wavelengths for laser thrombolysis: An absorption range of 100–1000 cm^{-1} corresponds to the waveband between 410–590 nm for thrombus absorption. Ablation efficiency is independent of wavelength in this range at pulse energies above threshold. Selectivity is still maintained due to low absorption by artery.
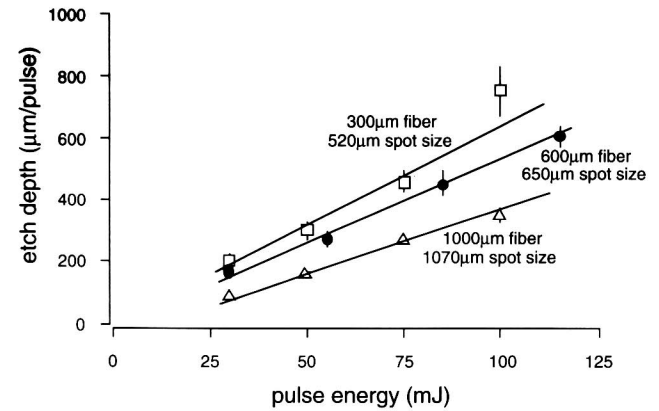
Fig. 8. Calculated etch depths at various pulse energies and fiber sizes: Ablated mass is assumed to be removed from a uniform cylinder with spot size as diameter. Etch depths represented here are an average of ten pulses. Absorption was 300 cm^{-1}. Error bars denote standard deviation of 10 samples. Lines are visual best fits.

Effect of Radiant Exposure

Radiant exposures produced by a 300 μm fiber (520 μm spot size) were about four times those produced by a 1000 μm fiber (1070 μm spot size) at similar energies, and yet ablation was more efficient with the larger fiber. Also, iso-radiant exposures did not result in similar ablation efficiencies. Thus there is no direct relationship between ablation efficiency and radiant exposure. Some previous studies have reported a linear increase in mass removal with radiant exposure [5,17,20]. However, in those studies the tissue was ablated in air and in an unconfined geometry. Further, the radiant exposure was varied by varying the pulse energy while maintaining a constant irradiated spot size. We also observed a linear increase in mass removal with pulse energy (constant ablation efficiency) for a single spot size. A possible explanation for the higher ablation efficiencies with larger fibers at the same energies could be that the dynamics of the vapor bubbles formed are different once the energy is above threshold.

Etch depths were calculated on the assumption that the ablated mass was removed from a cylindrical volume with the spot size as the diameter. The density of the gelatin was assumed to be 1 g/cm^3. Figure 8 shows the etch depth per pulse as a function of pulse energy for the three fibers used. It suggests that while smaller fibers take out less mass than bigger fibers at similar energies, they dig deeper craters into the target.

The ablation efficiencies measured in this study are in rough agreement with the ablation of calcified plaque and normal artery under saline as reported by Prince et al. [9]. However, they are about an order of magnitude higher than the results of other investigators who ablated tissue in air [8,17]. This again suggests that most of the work in the ablation process under a liquid is done by some mechanical action resulting from the vapor bubbles. Earlier studies have suggested the participation of the vapor bubble in tissue removal and damage. Van Leeuwen et al. and Jansen et al. investigated vapor bubbles as a potential cause of arterial dissections produced during excimer and holmium laser angioplasty [18,19].

Clinical Implications and Limitations

The results of this investigation indicate that laser wavelengths between 410–590 nm are most suitable for removing thrombus in vessels. Currently used wavelengths of 490 nm and 577 nm for laser thrombolysis were chosen because of good absorption by beta-carotene and hemoglobin respectively. As shown in this study, these are acceptable wavelengths from an ablation efficiency point of view. Choosing a wavelength must take other factors into consideration, e.g., cost and ease of design.

The higher ablation efficiencies with larger fibers at similar energies suggest that larger diameter catheters would be better for laser thrombolysis to create wider lumen. However, the size of the catheter would be limited by flexibility requirements and the size of the vessel. Also, larger

catheters would not dig as deeply into the thrombus as a small catheters at similar energies. Higher pulse energies result in greater ablation masses. The maximum energy that can be used with a particular spot size during laser thrombolysis would be limited by the ablation threshold for the vessel wall.

We have measured the ablation threshold as a function of absorption of gelatin—a phantom for thrombus. They suggest that the tissue needs to be heated to only 100°C for ablation to commence. There is also good agreement with the thresholds for thrombus and artery at similar absorptions. Since the choice of laser wavelength determines the absorption coefficients of thrombus and vessel wall, we can now predict the ablation threshold for thrombus and vessel wall at any wavelength in the visible region. The radiant exposure for laser thrombolysis can then be chosen such that it is above the threshold for thrombus, but below that of artery.

Current clinical trials use pulse energies of 50–60 mJ at a wavelength of 490 nm out of a 1 mm catheter. The absorption of thrombus at 490 nm is about 100 cm^{-1} and that of artery is less than 10 cm^{-1}. The currently used radiant exposure range of 60–75 mJ/mm^2 is about three times and half the ablation thresholds of thrombus and artery respectively and is therefore in the window for a safe and efficient therapy.

REFERENCES

1. Grundfest WS, Litvack F, Forrester JS, T. Goldenberg HJCS, Morgenstern L, Fishbein M, McDermid IS, Rider DM, Pacala TJ, Laudenslager JB. Laser ablation of human atherosclerotic plaque without adjacent tissue injury. J Am Coll Cardiol 1985; 5:929–933.
2. Grundfest WS, Litvack IF, Goldenberg T, Sherman T, Morgenstern L, Carroll R, Fishbein M, Forrester J, Margitan J, McDermid S, Pacala T, Rider DM, Laudenslager JB. Pulsed ultraviolet lasers and the potential for safe laser angioplasty. Am J Surg 1985; 150:220–226.
3. Gregory K. Laser thrombolysis. In: Topol EJ, ed. "Interventional Cardiology.", Chap. V, W.B. Saunders Company 1994. Philadelphia, PA. Volume 2, 2. edition. pp 892–902.
4. Singleton DL, Paraskevopoulos G, Taylor RS, Higginson LAJ. Excimer laser angioplasty: Tissue ablation, arterial response, and fiber optic delivery. IEEE J Quantum Electron 1987; QE-23:1772–1781.
5. Litvack F, Grundfest WS, Goldenberg T, Laudenslager J, Pacala T, Segalowitz J, Forrester J. Pulsed laser angioplasty: Wavelength power and energy dependencies relevant to clinical application. Lasers Surg Med 1988; 8:60–65.
6. Jansen ED, Le TH, Welch AJ. Excimer, Ho:YAG, and Q-switched Ho:YAG ablation of aorta: a comparison of temperatures and tissue damage in vitro. Appl Opt 1993; 32:526–534.
7. Xie DY, Hassenstein S, Oberhoff M, Hanke H, Baumbach A, Hohla K, Haase KK, Karsh KR. in vitro evaluation of ablation parameters of normal and fibrous aorta using smooth excimer laser coronary angioplasty. Lasers Surg Med 1993; 13:618–624.
8. Prince MR, Deutsch TF, Shapiro AF, Margolis RJ, Oseroff AR, Fallon JT, Parrish JA, Anderson RR. Selective ablation of atheromas using a flashlamp-excited dye laser at 465 nm. Proc Natl Acad Sci USA 1986; 83:7064–7068.
9. Prince MR, LaMuraglia GM, Teng P, Deutsch TF, Anderson RR. Preferential ablation of calcified arterial plaque with laser-induced plasmas. IEEE J Quantum Electron 1987; QE-23:1783–1786.
10. LaMuraglia GM, Anderson RR, Parrish JA, Zhang D, Prince MR. Selective laser ablation of venous thrombus: Implications for a new approach in the treatment of pulmonary embolus. Lasers Surg Med 1988; 8:486–493.
11. LaMuraglia GM, Prince MR, Nishioka NS, Obremski S, Birngruber R. Optical properties of human arterial thrombus, vascular grafts, and sutures: Implications for selective laser thrombus ablation. IEEE J Quantum Electron 1990; 26:2200–2206.
12. van Leeuwen T, van der Veen MJ, Verdaasdonk RM, Borst C. Noncontact tissue ablation by Holmium:YSGG laser pulses in blood. Lasers Surg Med 1991; 11:26–34.
13. Rink K, Delacrétaz G, Salathé RP. Fragmentation process induced by microsecond laser pulses during lithotripsy. App Phys Lett 1992; 61:258–260.
14. Vogel A, Schweiger P, Frieser A, Asiyo MN, Birngruber R. Intraocular Nd:YAG laser surgery: Light-tissue interaction, damage range, and reduction of collateral effects. IEEE J Quantum Electron 1990; 26:2240–2259.
15. Tomaru T, Geschwind HJ, Boussignac G, Lange F, Tahk SJ. Comparison of ablation efficiency of excimer, pulsed dye, and holmium-YAG lasers relevant to shock waves. Am Heart J 1992; 123:886–895.
16. Partovi F, Izatt JA, Cothren RM, Kittrell C, Thomas JE, Strikwerda S, Kramer JR, Feld MS. A model for thermal ablation of biological tissue using laser radiation. Lasers Surg Med 1987; 7:141–154.
17. Walsh Jr. JT, Deutsch TF. Pulsed CO_2 laser ablation of tissue: Effect of mechanical properties. IEEE Trans Biomed Eng 1989; 36:1195–1201.
18. van Leeuwen T. Bubble formation during pulsed mid-infrared and excimer laser ablation: Origin and implications for laser angioplasty. Ph.D. thesis, Rijksuniversiteit te Utrecht, 1993.
19. Jansen ED. Pulsed laser ablation of biological tissue: In-

fluence of laser parameters and tissue properties on thermal and mechanical damage. Ph.D. thesis, University of Texas at Austin, 1994.

20. Strikwerda S, Bott-Silverman C, Ratliff NB, Goormastic M, Cothren RM, Costello B, Kittrell C, Feld MS, Kramer JR. Effects of varying argon ion laser intensity and exposure time on the ablation of atherosclerotic plaque. Lasers Surg Med 1988; 8:66–71.